

Generalizations on Compartment Fires from Small-scale Experiments for Low Ventilation Conditions

YUNYONG UTISKUL, and JAMES G. QUINTIERE

Department of Fire Protection Engineering
University of Maryland at College Park
0151 Martin Hall (Engineering Building)
College Park, Maryland 20742, USA

ABSTRACT

Some generalizations on compartment fires, the dimensionless plots of the initial peak pressure and the time to extinction, are presented using data from small-scale experiments favoring low ventilation conditions. Two regimes of behavior are found: (1) Early, pressurized fires leading to extinction, and (2) Quasi-steady fires and flow conditions. Oscillating fires occur at the transition between (1) and (2). A critical value of Q^* was found for this transition. A theoretical analysis to support the experimental critical value was shown. A relationship for the oxygen concentration in the upper and the lower part layer was examined. This enabled an estimation of the mixing between the upper layer and the inlet vent flow. In ventilation-limited fires, the behavior of a limited area of fuel surface in flames was analyzed.

KEYWORDS: compartment fires, extinction, filling, limited burning, oscillating flames

NOMENCLATURE LISTING

A	Area	Y	Mass fraction
c_p	Specific heat	ϕ	Equivalence ratio
C_d	Flow coefficient	λ	Heat loss factor
f	Mixing Ratio	ρ	Density
f	Function of	τ	Dimensionless time
g	Gravity	Subscripts	
H	Compartment Height	b	Burn
L	Heat of gasification	$fill$	Filling
\dot{m}	Mass flow rate	f	Flame
P	Pressure	F	Fuel
P	Dimensionless pressure	l	Lower
\dot{Q}	Energy release rate	L	Loss
Q^*	Dimensionless energy	mix	Entraining from upper layer
r	Stoichiometric oxygen to fuel mass ratio	o	Ambient or Opening
S	Compartment floor area	ox	Oxygen
s	Stoichiometric air to fuel mass ratio	p	Pressure
T	Temperature	u	Upper
t	Time		
Y	Mass fraction		

INTRODUCTION

A number of experimental studies on compartment fires [1-3] have been conducted and revealed interesting phenomena such as oscillating flames, and vent flames (under ventilation limited burning). A method to characterize these behaviors based on ventilation has been presented [4]; however, a complete generalization of compartment fires using currently available data has yet to be determined and fully understood. This paper will present some generalizations from recent small-scale experimental data [3] by using rather simple but powerful dimensionless presentations to display some physics of the compartment fire behavior.

Two main modes of burning in low ventilation compartment fires have been recognized. The first is the case where the flame goes to extinction for small vents, and the second, the case where all the fuel burns to completion for large vents. In the latter case, we have quasi-steady burning. An analysis to compute the critical value to indicate the transition between the two modes will be presented and compared to experimental results.

For ventilation-limited conditions in a long aspect geometry compartment, flames moving from the front (near vent) towards the rear of enclosure were observed during quasi-steady burning [5]. An investigation of this behavior will also be presented based on an analysis of burning on partial fuel area due to ventilation-limited condition.

EXPERIMENT

Description

The experimental apparatus is shown in Fig. 1. The compartment was built with 2.54 cm thick Type-M Kaowool® board. All joints were sealed using fire resistant sealant to ensure no unintended leaks. The compartment has the feature of increasing the depth and changing the location of the fuel between the far end and vent end. In the current study two sizes of compartment were considered and referred to as the “cubic” and the “long box”. They are in size of 40x40x40 cm and 40x40x120 cm (width x height x depth) respectively. For the cubic box, the fuel was located at the centre of the box. In the long box, the fuel pan is located either near the vent or near the rear wall. The wall vent arrangement consisted of equal area vents at the top and bottom of heights 1 to 3 cm. The total area of the top and bottom wall vents was varied from 2 to 240 cm². Heptane fuel (C₇H₁₆) was burned in a modified Pyrex® glass container with diameters of 6.5, 9.5, 12.0, and 19.0 cm. Measurements comprise fuel mass loss, gas temperature, differential pressure, heat flux, and mole fraction of oxygen, carbon monoxide, and carbon dioxide. The details of the measurements are described elsewhere [3,4]. Pressure differential and oxygen concentration measurements near the floor are featured herein.

Observation

There are four distinct regimes of burning behavior observed in this study. Regime 1, *extinction due to filling*, covers the cases where the vent size is small and the fire becomes extinguished because the compartment is filled nearly completely with smoke and the air supply is not sufficient to sustain a sufficient oxygen concentration. In addition, the flame stood upright, not affected by airflow, since during “filling” the vent flow is outward. In Regime 2, extinction also occurs due to insufficient oxygen. But in this regime, there is inflow from the lower vent which pushes the flame and it departs from the liquid fuel. *Oscillating* and *ghosting* flames are seen in this regime and usually

take place before flame extinction. A ghosting flame is a flame that lifts-off the liquid fuel surface and floats somewhat aimlessly away from the surface. *Oscillating flames* represent the condition where the flame is shrinking to extinction, but cycles back to its original size. This is repeated. In Regime 3, sustained steady oscillations are noted with no extinction until burnout. *Burning at the vent* is also observed in Regime 2 and 3. This is the classical ventilation-limited burning case where all of the oxygen of the incoming air is burned completely. In Regime 4, the fire burns steadily until the fuel is exhausted. This regime is marked by nearly *steady burning*.

These Regimes comprise two basic modes of fire and flow behavior. In Mode 1 (Regimes 1-3), filling forces all the flow out of the compartment (see the theory by Zukoski [6]). In Mode 2 (Regimes 2-4), quasi-bidirectional steady flow occurs. The oscillating Regimes 2 and 3 alternate between Modes 1 and 2. We shall examine the dynamics of these Modes.

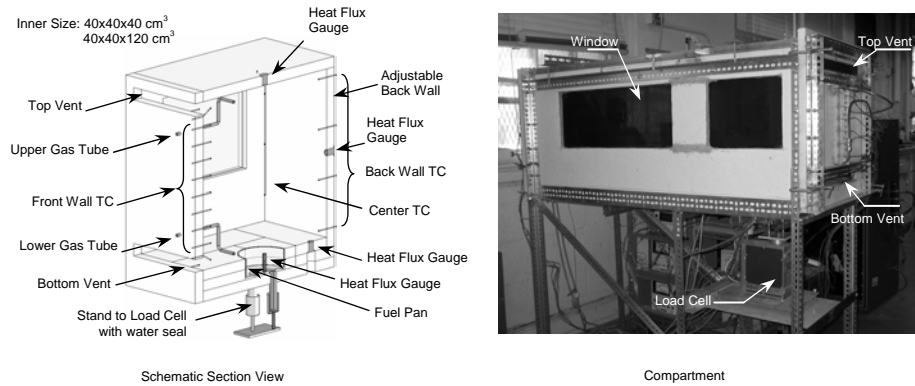


Fig. 1. Experimental apparatus.

PRESSURE RISE IN COMPARTMENT AND PRESSURE RESPONSE TIME

Consider here the initial state of the burning in the compartment and the pressure rise due to fire. The pressure near the floor will determine whether Mode 1 or 2 occurs. Assume uniform properties for gas inside the compartment and one directional outflow. From the conservation of energy, we have

$$\frac{V}{\gamma-1} \frac{dP}{dt} + \dot{m} c_p T_o = \dot{Q} - \dot{Q}_L = \dot{Q}_{net}. \quad (1)$$

Here, we have simplified the out flow at the initial temperature, T_o , for both vents. Dividing by \dot{Q}_{net} and inserting $\rho_o gH$, where H is the compartment height, yields

$$\frac{V}{\gamma-1} \frac{\rho_o gH}{\dot{Q}_{net}} \frac{d}{dt} (\Delta P / \rho_o gH) + \frac{\dot{m} c_p T_o}{\dot{Q}_{net}} = 1. \quad (2)$$

The vent flow rate occurring due to hydrostatic pressure differences can be given as $\dot{m} = \rho_o C_d A_o \sqrt{2\Delta P / \rho_o}$. Let $P = \Delta P / \rho_o g H$, and $\tau_p = t / t_p$ where the pressure characteristic time, $t_p = V \rho_o g H / (\gamma - 1) \dot{Q}_{net}$. Then Eq. 2 reduces to

$$\frac{dP}{d\tau_p} + \left(\frac{\sqrt{2} C_d}{Q^*} \right) \sqrt{P} = 1, \quad \text{where } Q^* = \dot{Q}_{net} / A_o \rho_o c_p T_o \sqrt{g \sqrt{H}} \quad (3)$$

For a cubic 40 cm compartment with the approximated \dot{Q} of 5 kW, the pressure characteristic time, t_p , is equal to 0.15 sec which indicates that the response time of the pressure is small. If the pressure responds quickly, $\frac{dP}{d\tau_p} \approx 0$ also C_d is equal to 0.68, then Eq. 3 reduces to

$$P = \Delta P / \rho_o g H = 1.08 (Q^*)^2 \quad (4)$$

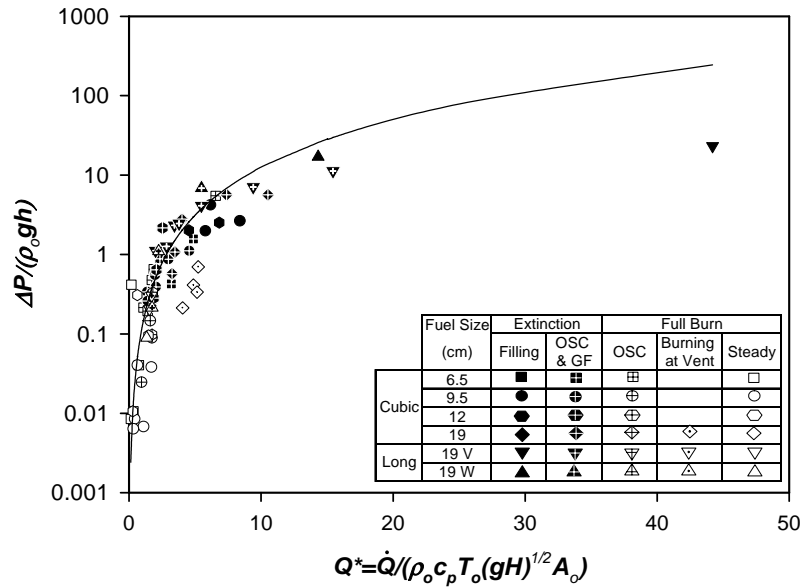


Fig. 2. Peak pressure dependence on Q^* .

In Fig. 2 the initial peak pressure, ΔP , from the experiment is plotted against the dimensionless energy release rate, Q^* . The peak pressure differential, ΔP , was measured by the pressure transducer near the bottom vent. Here we use Q^* in terms of \dot{Q}_{net} and $\dot{Q}_{net} = \dot{m}_F \Delta h_c$, where \dot{m}_F is the fuel mass loss rate measured in the experiment. The time when the peak pressure occurs was recorded in our database and found that the time scale was inversely proportional to \dot{Q} (not shown here). The filled symbols represent observed

extinction, while open symbols mean the liquid fuel was completely exhausted. The symbols (both filled and open) with plus sign (+) represent observed oscillating flames, and open symbols with dot inside refer to vent burning. In the legend table, the abbreviation V means the case where the fuel pan is located close to the vent, while W means the fuel pan is located near the back wall. The solid curve represents Eq. 4 with $\dot{Q}_{net} = \dot{Q}(1 - \lambda)$, and assuming the heat loss factor as $\lambda = 0.7$. It is clear from Fig. 2 that the higher Q^* , the higher initial peak pressure. In other words, we have high pressure for extinction cases (small vent), while the steady burning (large vent) gives much lower initial peak pressure. There are some discrepancies between the experiment and the theory at higher Q^* . We believe the discrepancy is due to a very small characteristic time at high \dot{Q} that is faster than the time response of the pressure transducers. Nevertheless, the experimental results agree well with the trend suggested by the theory.

SMOKE FILLING

The filling process is observed to be the initial flow behavior in the compartment fire. In our experiment, this becomes apparent when the differential pressure signals are examined, that is ΔP measured near top and bottom vents are positive values. Zukoski [6] has developed an analytical model to estimate the time required to fill a room with smoke. We will employ his analysis to investigate the filling behavior of our two-wall-vent case using a nondimensional filling time, $\tau_{fill} = t_{fill} \sqrt{g/H} (H^2/S)$, where S is the floor area, and another dimensionless parameter, $Q_{fill}^* = \dot{Q} / \rho_o c_p T_o \sqrt{g} H^{5/2}$.

These two dimensionless parameters are plotted in Fig. 3. Here the meaning for symbols is similar to what we have in the peak pressure plot. Time to fill, t_{fill} , is the time in the experiment when the thermocouple located at the 15% of the compartment height reads above 70°C. The dash-curve represents an approximated contour line of Q^* which then implies that these plots do not collide on the same curve because they represent different Q^* . In other words, the case where we have big vents or small fire does not fill. The solid curve is derived from Zukoski's theoretical model for the single ceiling leak case. Obviously there are differences between single-ceiling-leak and two-wall-vent filling process; however, the theory does span the range of these data.

EXTINCTION DUE TO SMOKE FILLING

Consider a compartment filling with smoke and only outward flow across the vent is present. The conservation of oxygen is given as

$$\rho_o V \frac{dY_{ox}}{dt} + \dot{m} Y_{ox} = - \frac{\dot{Q}}{\Delta h_{ox}}. \quad (5)$$

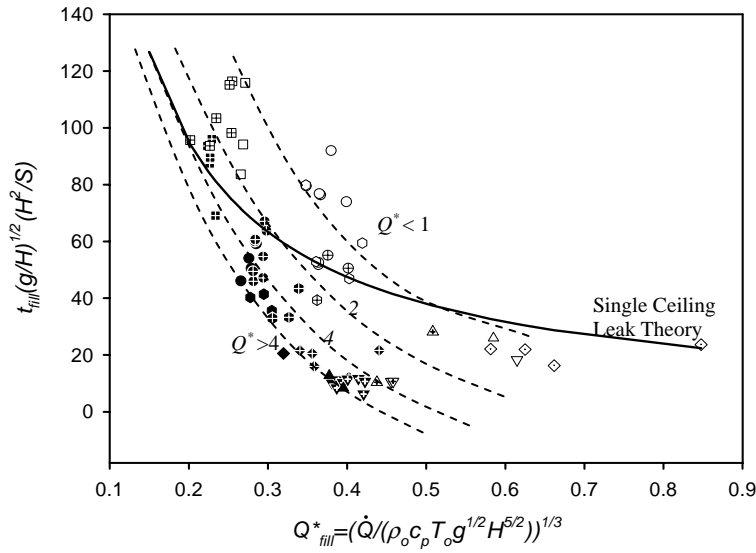


Fig. 3. Dimensionless filling time vs Q_{fill}^* .

Again, we evaluate the compartment density at the initial value for simplicity. From previous section we observe that pressure reaches its steady state very fast. Hence, we now assume that the rate of pressure rise in the compartment is equal to zero thereafter and Eq. 1 becomes

$$\dot{m} = \dot{Q}_{net} / c_p T_o . \quad (6)$$

Divide Eq. 10 by Eq. 11 to make dimensionless, we have

$$\frac{c_p T_o \rho_o V}{\dot{Q}_{net}} \frac{dY_{ox}}{dt} + Y_{ox} + \frac{\dot{Q} c_p T_o}{\dot{Q}_{net} \Delta h_{ox}} = 0 \quad (7)$$

Let $\Psi = Y_{ox} + (\dot{Q} c_p T_o) / (\dot{Q}_{net} \Delta h_{ox})$, and define dimensionless time as $\tau = \dot{Q}_{net} t / \rho_o c_p T_o V$. From Eq. 7 we have

$$\frac{d\Psi}{d\tau} + \Psi = 0 , \text{ and } \Psi = \Psi_o e^{-\tau} \quad (8)$$

By considering the initial state at ambient conditions and the final state at extinction, we can determine the dimensionless extinction time,

$$\tau_{ext} = - \left[\ln \left(\frac{Y_{ox,ext} + \dot{Q} c_p T_o / \dot{Q}_{net} \Delta h_{ox}}{0.233 + \dot{Q} c_p T_o / \dot{Q}_{net} \Delta h_{ox}} \right) \right]. \quad (9)$$

The oxygen mass fraction at extinction, $Y_{ox,ext}$, is approximately in the range of 0.09 - 0.15 [3,7]. This suggests that if there is extinction, τ_{ext} is a constant. Hence, the extinction time can be given as $t_{ext} = C(\rho_o c_p T_o V / \dot{Q}_{net})$.

In Fig. 4 the dimensionless time, τ , is plotted by substituting the time recorded when oscillating or ghosting flame started, and when extinction occurred. The filled symbols here mean the dimensionless time calculated using the time recorded when extinction took place, while the filled symbols with plus sign (+) represent the dimensionless time recorded when the oscillating flame or ghosting flame occurred. Furthermore, the open symbols with plus sign (+) mean the dimensionless time determined with the time recorded when sustained steady-oscillating flame started. It should be noted that there could be more than one data point in Fig. 3 that are from the same test. This graph shows the recorded times when several behaviors occur. Plots for the dimensionless time when the fuel was exhausted in steady burning are also included and presented by the open symbols. However, these data should not be considered extinction due to lack of oxygen, and the time for burning cessation depends on the quantity of the liquid fuel.

It can be seen in Fig. 4 that the dimensionless time when extinction occurs is relatively constant for Q^* larger than 4 or when we are in Regime 1; however, we may observe some variation of extinction time when Q^* is less than 4 as it approaches Regime 2 and 3. This supports the theoretical result that dimensionless extinction time, τ_{ext} is a constant. The border line between full-burn and extinction are also indicated here at $Q^* \sim 1.4$.

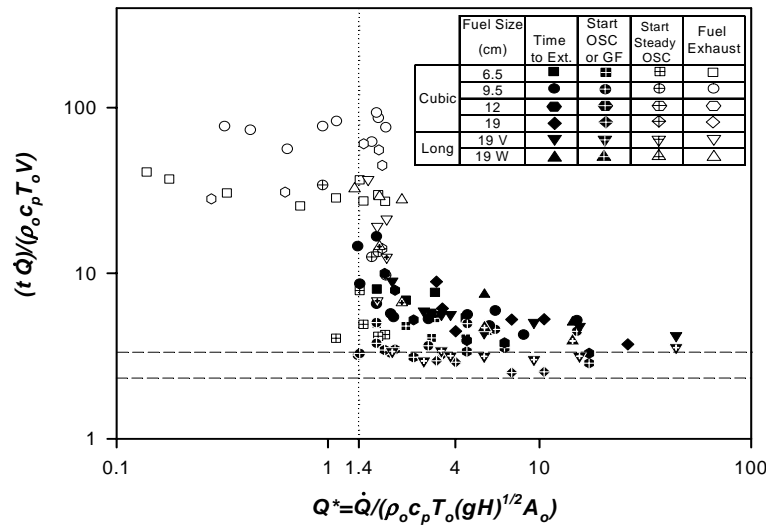


Fig. 4. Dimension less time vs. Q^* .

BREAK POINT BETWEEN EXTINCTION AND STEADY BURNING

Recall from Eq. 7 and consider now the steady state of the oxygen in the compartment. The transient term vanishes and we have

$$Y_{ox} = - \left(\frac{c_p T_o}{\Delta h_{ox}} \right) \frac{\dot{Q}}{\dot{Q}_{net}}. \quad (10)$$

This is physically impossible and shows that the flow must reverse at some point before extinction if the fire is to move to the steady burning regime. In other words, if flow reverses, we have at steady state (see Fig. 5).

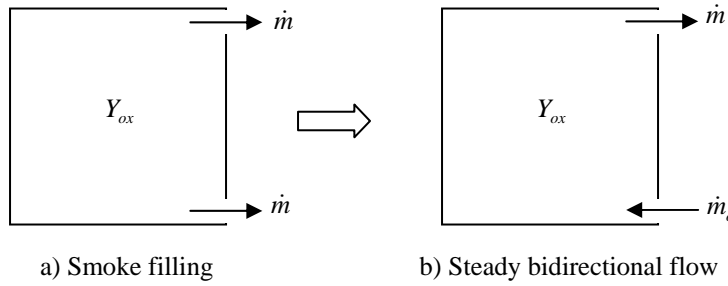


Fig. 5. Change of flow direction.

Therefore, the conservation of oxygen is now given as

$$\dot{m}(Y_{ox} - 0.233) = - \frac{\dot{Q}}{\Delta h_{ox}}. \quad (11)$$

If we assume well-mixed-filled state, but examine extinction at $Y_{ox,ex} \sim 0.09-0.15$. Equation 11 can be considered on the interface between “smoke filling” and “steady bidirectional flow”. We must have \dot{m} such that

$$\dot{m} = \frac{\dot{Q}}{(0.233 - Y_{ox,ex}) \Delta h_{ox}}. \quad (12)$$

This implies that if \dot{m} is smaller than the value determined by Eq. 12, the fire should go to extinction. By substituting \dot{m} with $\dot{m} = K \rho_o \sqrt{g} A_o \sqrt{H}$ where $K = 0.5 \sqrt{2} C_d \cdot f(T_o/T)$ [4], we obtain a critical value for extinction from Eq. 12

$$\left[\frac{\dot{Q}}{K \rho_o \sqrt{g} A_o \sqrt{H} \Delta h_{ox}} \right]_{crit} = (0.233 - Y_{ox,ex}). \quad (13)$$

$$\left[Q^* \left(\frac{c_p T_o}{\Delta h_{ox} K} \right) \right]_{crit} = 0.08 \text{ to } 0.14 \quad (14)$$

If $Q^* (c_p T_o / \Delta h_{ox} K)$ exceeds its critical value, then we have extinction. Based on the range of maximum gas temperature measured from the experiment we can estimate the average maximum value for $f(T_o/T)$ as 0.41 (See Fig. 6). Solving for Q^* using Eq. 14 with $f(T_o/T) = 0.41$ and the critical value of 0.14, we obtain Q^* at the break-point between extinction and full burn ~ 1.0 compared to 1.4 which is what we have observed experimentally in Fig. 4.

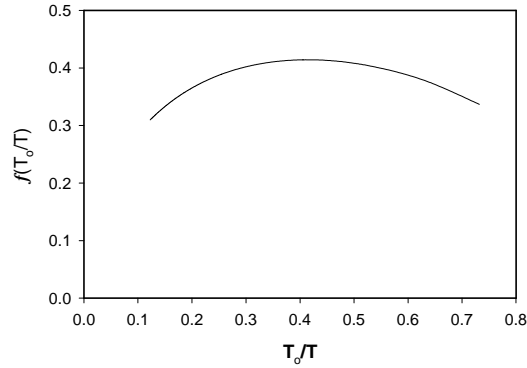


Fig. 6. Variation of $f(T_o/T)$.

RELATIONSHIP FOR UPPER AND LOWER OXYGEN

We now proceed our discussion with the assumption of stratified gas in the compartment and bi-directional flow (Mode 2) in order to investigate the relationship of the oxygen in upper and lower portion of the compartment. Consider the control volume I and II in a stratified compartment. From conservation of oxygen we have

CV-I: Lower Zone

$$\dot{m}_o 0.233 + \dot{m}_{mix} Y_{ox,u} = (\dot{m}_o + \dot{m}_{mix}) Y_{ox,l} \quad (15)$$

$$Y_{ox,l} = \frac{0.233 + (\dot{m}_{mix} / \dot{m}_o) Y_{ox,u}}{1 + (\dot{m}_{mix} / \dot{m}_o)} \quad (16)$$

CV-II: Upper Zone

$$(\dot{m} + \dot{m}_{mix}) Y_{ox,u} - (\dot{m}_o + \dot{m}_{mix}) Y_{ox,l} = -(\dot{m}_{F,react}) r \quad (17)$$

where r is the stoichiometric oxygen to fuel mass ratio and $\dot{m} = \dot{m}_F + \dot{m}_o$. For fuel controlled fires, $\dot{m}_{F,react} = \dot{m}_F$, while for ventilation controlled fires, $\dot{m}_{F,react} = \dot{m}_o / r$. Subtracting Eq. 15 from 17 and rearranging yield

$$Y_{ox,u} = \frac{0.233 - r(\dot{m}_F/\dot{m}_o)}{1 + (\dot{m}_F/\dot{m}_o)} \text{ for } \phi < 1, \text{ and } Y_{ox,u} = 0 \text{ for } \phi \geq 1 \quad (18)$$

where ϕ is the equivalence ratio. Furthermore, define a mixing ratio as $f = \dot{m}_{mix} / \dot{m}_o$, and substitute Eq. 18 into Eq. 16. We have

$$\frac{Y_{ox,l}}{0.233} = \left(\frac{1}{1+f} \right) - \left(\frac{f}{1+f} \right) \left(\frac{1-\phi}{1+\phi/s} \right); \phi < 1, \text{ and} \quad (19)$$

$$\frac{Y_{ox,l}}{0.233} = \left(\frac{1}{1+f} \right); \phi \geq 1.$$

In Fig. 7, $(Y_{ox,l}/0.233)$ are plotted against ϕ . Here we calculate $\phi = \dot{m}_F s / \dot{m}_{air}$, where s is the stoichiometric air to fuel mass ratio, based on \dot{m}_F from experiment and estimated $\dot{m}_{air} = 0.5\sqrt{2}C_d\rho_o\sqrt{g}A_o\sqrt{H}f(T_o/T)$ with $f(T_o/T) = 0.41$. Since we are looking at the bi-directional flow mode (Fig. 5b), $Y_{ox,l}$ used in this plot are from the full-burn cases. Note that data from the ventilation limited cases (burning at the vent) are also included here. Eq. 19 is imposed on the plot to approximate the range of mixing ratio. The solid line is based on the mixing ratio of 3.2 and the dash line is from the mixing ratio of 0.8.

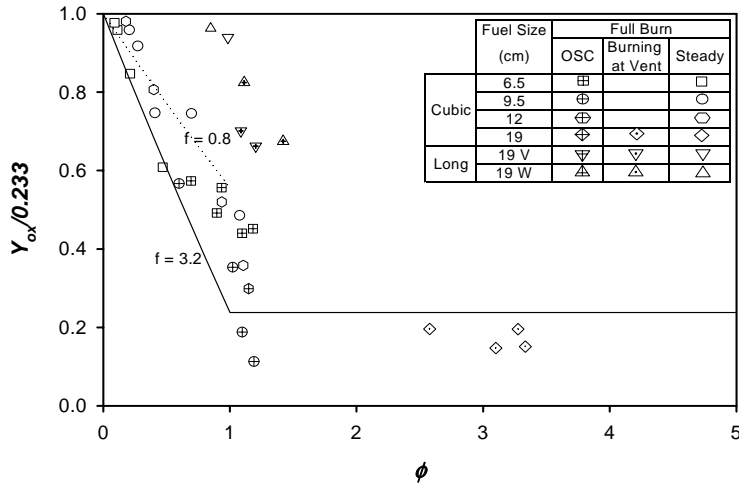


Fig. 7. Lower oxygen mass fraction vs. equivalence ratio.

BURNING AREA IN VENTILATION-LIMITED FIRE

Thomas and Bennetts [5] observed flames partially burning over a series of liquid fuel trays in their experimental study on long and wide enclosures. They reported that after ignition the flame formed itself at the front of the fuel tray closest to the vent. Later, when the fuel in the front tray was exhausted, the flame moved towards the rear of the enclosure (away from vent) to the next adjacent tray. This behavior takes place because the ventilation-limited condition occurs where burning is governed by the amount of supplied air. We also experienced the same behavior in our long compartment with distributed fuel pans over the floor. Motivated by such observations, we offer a reason that is that only a certain amount of fuel area will react with the limited amount of air supply. The flame therefore burns only on this certain area to match its needed fuel, and then “moves” when the local fuel is exhausted. The following analysis is put forth to estimate the burning area in ventilation-limited fire. For the ventilation-limited condition, we have

$$\dot{m}_b = \dot{m}_{air} / s \quad (20)$$

Here \dot{m}_b denotes the fuel mass that actually burns and s is the stoichiometric air to fuel mass ratio. The fuel supply rate in the compartment can also be estimated in terms of its burning rate in ambient air, \dot{m}_{∞}'' , [8] as

$$\dot{m}_b = \left[\dot{m}_{\infty}'' \frac{Y_{ox,l}}{0.233} + \frac{\sigma(1-\varepsilon_f)(T^4 - T_o^4)}{L} \right] A_b, \quad (21)$$

where T here denotes the upper gas temperature in the compartment, L is heat of gasification and A_b is the burning area. Combining Eq. 20 and 21 yields

$$A_b = \left(\frac{\dot{m}_{air}}{s} \right) / \left[\dot{m}_{\infty}'' \frac{Y_{ox,l}}{0.233} + \frac{\sigma(1-\varepsilon_f)(T^4 - T_o^4)}{L} \right]. \quad (22)$$

Generally, liquid pool fires in small-scale have flame of low absorptivity [8], hence ε_f can be neglected. The burning rate in ambient is also given as [9]

$$\dot{m}_{\infty}'' = \dot{m}_{\max}'' (1 - e^{-kD}). \quad (23)$$

The air flow rate can be estimated by $\dot{m}_{air} = K\rho_o\sqrt{g}A_o\sqrt{H}$ where the coefficient K changes depending on vent geometry. By using Eq. 22, and 23, one can now estimate the burning area in ventilation-limited condition.

Referred again to the study done by Thomas and Bennetts [5], we could try estimating the burning area in their wide enclosure case (1.5 m wide x 0.6 m depth x 0.3 high) with full opening size of 1.5 m x 0.275 m (width x height). By approximating the free burning rate

of $15 \text{ g/m}^2\text{s}$ [9], $s = 8.95$, $\dot{m}_{air} = 106.5 \text{ g/s}$ for single-wall-vent [9], and $(Y_{ox,l}/0.233) \sim 0.23$ using the mixing ratio of 3.2, we obtain the burning area approximately as 0.143 m^2 . According to Thomas and Bennetts, the behavior was two dimensional. Hence we assume the flame burns over the full width of the enclosure, 1.5 m; then the “depth” of the flame is approximately given as $0.143/1.5 = 0.095 \text{ m}$. Roughly checking with the picture provided in Thomas’s paper (Figure 5b, pp. 946 [5]), the flame depth is scaled to be about 0.08 m in apparent agreement with the computed value.

CONCLUDING REMARKS

This paper illustrates some aspects and generalizations of compartment fire behavior through dimensionless correlations. Although small scale data were used to generate these general results, they should be valid for larger scale systems provided the important physics has been included in the correlations. Heat loss effects have not been explicitly considered in terms of dimensionless and properties and these effects will limit the generality of the results. Other vent configurations could also influence these results.

REFERENCES

- [1] Takeda, H., and Akita, K., “Critical Phenomenon in Compartment Fires with Liquid Fuels,” *Proceeding of the 18th Symposium (International) on Combustion*, Combustion Institute, 1981, pp 519-527.
- [2] Chamchine, A.V., Graham, T.L. Makhviladze, G. M., Holmstedt, G., Snegirev, A. Yu., And Talalov, V.A., “Experimental Studies of Under-ventilated Combustion in Small and Medium-Scale Enclosures,” *Proceeding of the 4th International Seminar—Fire and Explosion Hazards*, 2003.
- [3] Utiskul, Y., Quintiere, J.G., Rangwala, A.S., Ringwelski, B.A., Wakatsuki, K., and Naruse, T., “Compartment Fire Phenomena Under Limited Ventilation,” *Fire Safety Journal*, **40**, pp. 367-390, (2005).
- [4] Utiskul, Y., and Quintiere, J.G., “Wall-vent Compartment Fire Behavior under Limited Ventilation,” *Interflam 2004—Proceedings of the 10th International Conference*, InterScience Communications, 2004, pp. 105-116.
- [5] Thomas, I.R., and Bennetts, I.D., “Fires in Enclosures with Single Ventilation Openings – Comparison of Long and Wide Enclosure,” *Fire Safety Science — Proceedings of the Sixth International Symposium*, International Association for Fire Safety Science, 2000, pp. 941-952.
- [6] Zukoski, E.E., “Development of a Stratified Ceiling Layer in the Early Stages of a Closed-Room Fire,” *Fire and Materials*, **2**, pp. 54-62, (1978).
- [7] Quintiere, J.G., and Rangwala, A.S, “A Theory of Flame Extinction Based on Flame Temperature,” *Fire and Materials*, **28**, pp. 387-402, (2003).
- [8] Quintiere, J.G., “Fire Behavior in Building Compartments,” *Proceeding of the Combustion Institute 29*, Combustion Institute, 2002, pp. 181-193.
- [9] Karlsson, B., and Quintiere, J.G., *Enclosure Fire Dynamics*, CRC Press, 2000, pp.33 & 99.